

Zerobot[®]: A Remote-controlled Robot for Needle Insertion in CT-guided Interventional Radiology Developed at Okayama University

Takao Hiraki^{a*§}, Tetsushi Kamegawa^b, Takayuki Matsuno^c, Toshiyuki Komaki^a,
Jun Sakurai^d, and Susumu Kanazawa^a

^aDepartment of Radiology, Okayama University Graduate School of Medicine, Dentistry and Pharmaceutical Sciences,

^dCenter for Innovative Clinical Medicine, Okayama University Hospital, Okayama 700-8558, Japan,

^bGraduate School of Interdisciplinary Science and Engineering in Health Systems, and

^cGraduate School of Natural Science and Technology, Okayama University, Okayama 700-8530, Japan

Since 2012, we have been developing a remote-controlled robotic system (Zerobot[®]) for needle insertion during computed tomography (CT)-guided interventional procedures, such as ablation, biopsy, and drainage. The system was designed via a collaboration between the medical and engineering departments at Okayama University, including various risk control features. It consists of a robot with 6 degrees of freedom that is manipulated using an operation interface to perform needle insertions under CT-guidance. The procedure includes robot positioning, needle targeting, and needle insertion. Phantom experiments have indicated that robotic insertion is equivalent in accuracy to manual insertion, without physician radiation exposure. Animal experiments have revealed that robotic insertion of biopsy introducer needles and various ablation needles is safe and accurate *in vivo*. The first *in vivo* human trial, therefore, began in April 2018. After its completion, a larger clinical study will be conducted for commercialization of the robot. This robotic procedure has many potential advantages over a manual procedure: 1) decreased physician fatigue; 2) stable and accurate needle posture without tremor; 3) procedure automation; 4) less experience required for proficiency in needle insertion skills; 5) decreased variance in technical skills among physicians; and 6) increased likelihood of performing the procedure at remote hospitals (*i.e.*, telemedicine).

Key words: robot, needle insertion, CT-guided interventional radiology

Computed tomography (CT)-guided interventional procedures are performed by inserting a specific needle into a lesion under CT-guidance. Such procedures include ablation, biopsy, drainage, preoperative marking, *etc.* CT-guided procedures are more advantageous than surgical approaches because they are faster, less invasive, and less costly. The advent of the CT fluoroscopic system dramatically changed CT-guided interventional procedures. This system enables

the physician to perform CT scanning, with near real-time image display, anytime during a procedure by pressing a foot switch; thereby, the procedure time is further decreased. However, physician intraprocedural radiation exposure may be a major concern, as the procedure usually requires the physician to be positioned near the CT scanner during needle insertion (Fig. 1). We previously evaluated physician radiation exposure during CT fluoroscopy-guided renal cryoablation (CRA) and lung radiofrequency ablation (RFA) [1]. The

Received July 23, 2018; accepted August 27, 2018.

*Corresponding author. Phone: +81-86-235-7313; Fax: +81-86-235-7316
E-mail: takaoh@tc4.so-net.ne.jp (T. Hiraki)

[§]The winner of the 2017 Incentive Award of the Okayama Medical Association in General Medical Science.

Conflict of Interest Disclosures: Drs. Hiraki and Kanazawa received a grant for work related to this study from Cannon Medical Systems. The other authors declare no conflicts of interest.



Fig. 1 A conventional computed tomography (CT) fluoroscopy-guided interventional procedure. The physician stands near the CT gantry to hold the needle (arrowhead) using plastic forceps (white arrow). The black arrow indicates the CT gantry controller.

operator's mean effective dose per procedure was 6.1 μ Sv during renal CRA and 0.7 μ Sv during lung RFA; the mean equivalent dose to the operator's finger skin per procedure was 2.1 mSv during renal CRA and 0.3 mSv during lung RFA.

Therefore, we hypothesized that a remotely controllable robot capable of performing needle insertions could eliminate physician radiation exposure. Since 2012, we have been developing a robot with this capability, along with medical-engineering cooperation and industry-academia collaboration [2-11]. In addition to eliminating physician radiation exposure, this robotic procedure has other potential advantages over the traditional manual procedure including: decreased physician physical fatigue, which occurs due to the sitting posture required for performing the procedure; stable and accurate needle posture without tremor, which may facilitate three-dimensional needle insertion (*i.e.*, off-CT plane insertion); procedure automation, which could decrease procedure time and patient radiation exposure; less experience required for proficiency in needle insertion skills; decreased variance in needle insertion skills among physicians; and increased likeli-

hood of performing the procedure at remote hospitals (*i.e.*, telemedicine).

Related Work by Other Researchers

Several commercially available robots for CT-guided intervention have been developed, including iSYS (Kitzbuhel, Austria) [12-14], Innomotion (Innomedic, Herxheim, Germany) [15-19], and Maxio (Perfint Healthcare, Chennai, India) [20-23]. iSYS and Innomotion are table-mounted robots, while Maxio is a large floor-mounted robot. The tasks of these robots are limited to needle path planning, needle positioning, needle orientation, and needle insertion guidance. Unlike our robot, these robots cannot perform the needle insertion; a physician must insert the needle manually.

Several robots have been developed that can perform needle insertions. Among those, AcuBot, a table-mounted robot with six degrees of freedom (DOF), has been the most extensively developed [24-28]. Acubot has been used in clinical interventional procedures (*e.g.*, ablation, biopsy, and nephrostomy) [24-26]; however, it has yet to be commercialized. Other robots used for needle insertion under CT-guidance are still used in laboratories only. A light puncture robot (LPR) has a specific structure composed of a patient-mounted needle holder supported by a specific frame [29]. Robopsy is a compact disposable patient-mounted robot [30]. Won *et al.* modified a floor-mounted manufactured robot to enable needle insertion, which is controlled using a master-slave system [31]. Shahriari *et al.* proposed a robot that would enable needle insertion under real-time fusion images of CT and electromagnetic data [32]. XACT Robotics, Ltd (Caesarea, Israel) developed a patient-mounted robot that enables needle insertion during stepwise correction of needle orientation [33].

Zerobot[®]

The robotic system (Zerobot[®]) was designed at Okayama University (Okayama, Japan) and manufactured by Medicalnet Okayama (Okayama, Japan). The system consists of a robot (Fig.2) and an operation interface (Fig.3). The tasks of the robot are to hold, locate, orient, and insert a needle under CT-guidance. The physician manipulates the robot to perform these

tasks using the interface. The size of the robot and the system configuration are shown in Fig.2 and Fig.4, respectively. The robotic system is not commercially

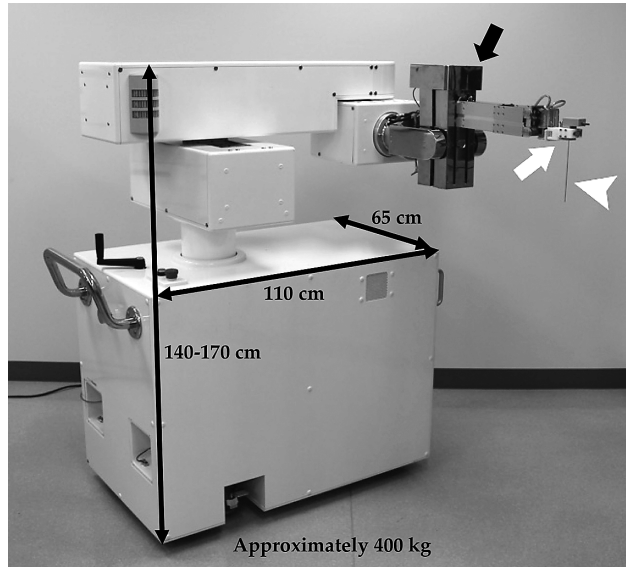


Fig. 2 The Zerobot®. The robot consists of a manipulator on a base. The manipulator includes an arm with an attached needle holder (white arrow). The needle (arrowhead) is attached to the holder. The black arrow indicates the linear guide mechanism for needle insertion. The base dimensions are 65 cm × 110 cm; the height is 140–170 cm; the weight is approximately 400 kg.

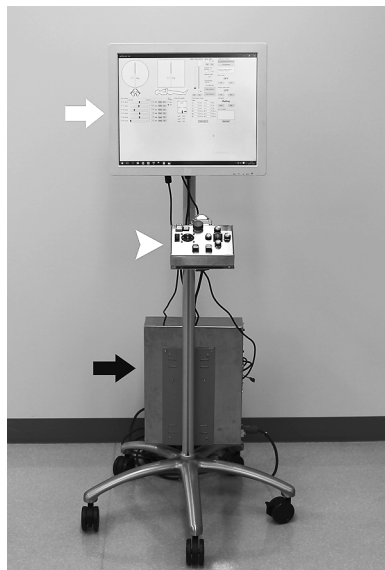


Fig. 3 Operation interface. The operation interface is comprised of a portable controller (arrowhead), a touch-screen (white arrow), an operation PC (black arrow), and a mobile platform.

available at this time.

Robot. The robot is floor-mounted and specifically designed for use with sliding gantry CT scanners for interventional procedures. Thus, the robot will not fit most conventional (*i.e.*, sliding table) CT scanners. The robot consists of a manipulator on a base (Fig. 2). The manipulator includes an arm, constructed using a parallel link mechanism (Fig. 2). At the end of the arm, a needle is attached to a needle holder (Fig. 2). The robot is mobile, having four wheels on the base; thus, it is placed beside the CT table. The end of the arm is compact and can fit within a 72 cm diameter CT bore. The arm can be rotated axially, allowing the robot to be positioned on either side of the CT table (Fig. 5). Furthermore, the arm can be removed from the opera-

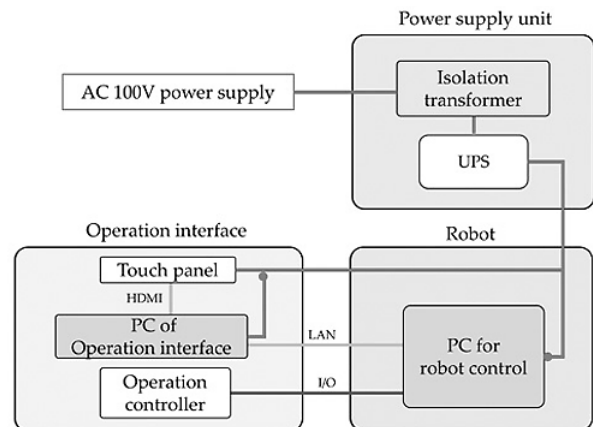


Fig. 4 System configuration. AC, alternating current; UPS, uninterruptible power supply; LAN, local area network; HDMI, high-definition multimedia interface; I/O, input/output.

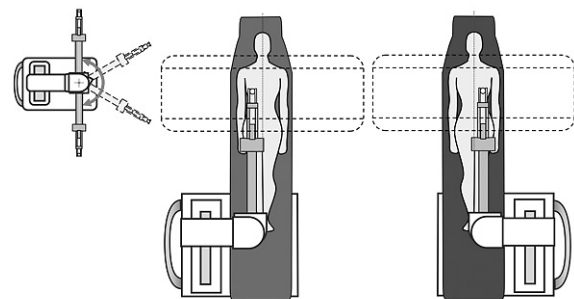


Fig. 5 Arm rotation and robot positioning. The robot arm can be rotated axially, allowing the robot to be positioned on either side of the computed tomography (CT) table. Therefore, the robot can be positioned at the side of the CT table that coincides with the side of the patient where the needle will be inserted.

tive field immediately in case of emergency. Two force sensors are attached to the arm end to provide the physician with force and torque data.

The needle holder will fit the proximal end of many commercially available needles; thus, a specific type of needle is not required. Currently, needle holders are available for each of the following needles: the biopsy introducer needle (TASK Laboratory, Tochigi, Japan) (Fig. 6), the Cool-tip RFA needle (Covidien, Mansfield, MA), the LeVein RFA needle (Boston Scientific Corporation, Spencer, IN), the IceRod CRA needle (Galil Medical Ltd, Yokneam, Israel), and the Emprint microwave ablation (MWA) needle (Covidien). The needle holders are made of engineering plastic to avoid metal artifact and endure autoclave sterilization.

The robot is based on a serial-link mechanism with six DOF: two rotational DOF around the A- and B-axes for needle orientation; three linear DOF along the X-, Y-, and Z-axes for needle location; and one linear DOF

along the P-axis for needle insertion and removal (Fig. 7). Needle insertion and removal is enabled using a linear guide mechanism (Fig. 2). The range of each axis motion is shown in Fig. 7. A remote center of motion (RCM) function is available for needle orientation, allowing the needle angle to change around a predefined pivot point, usually set at the needle tip (Fig. 8). This motion is enabled by the collaborative motion of the Y- and Z-axes, accompanied by A-axis motion for lateral needle angulation, and by the collaborative motion of the X- and Z-axes, accompanied by B-axis motion for craniocaudal needle angulation.

Each DOF may be driven in either slow or fast mode. In addition, an ultrafast insertion (approximately 500 mm/sec), achieved by a pneumatic actuator, is also available; it is usually used for insertion toward the skin and for movable targets.

Operation interface. The operation interface is comprised of a portable controller, a touch screen, an operation PC, and a carriage (Fig. 3). The operation PC

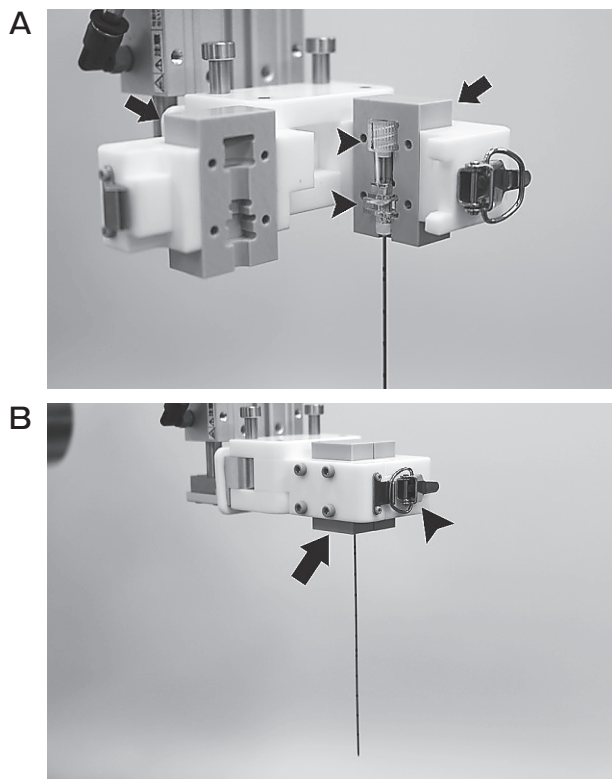


Fig. 6 The needle holder for the biopsy introducer needle. (A) The plastic needle holder (arrows) is specifically designed to fit the proximal end of the biopsy introducer needle (arrowheads). (B) The needle holder (arrow) is closed with a draw latch (arrowhead) to secure the biopsy introducer needle.

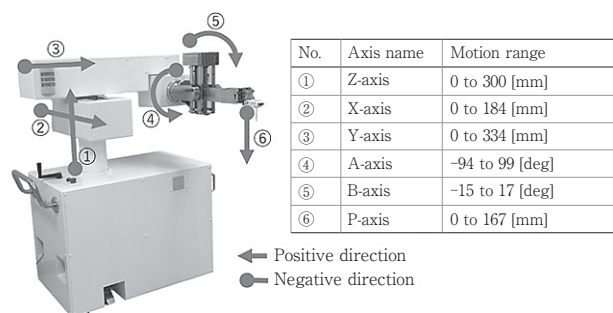


Fig. 7 The axes and degrees of freedom (DOF). The motion range of each DOF is shown in the table.

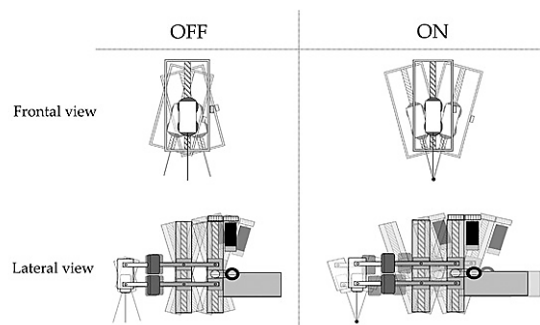


Fig. 8 The remote center of motion (RCM) function. The RCM function enables altered needle orientation around the needle tip (right). When the function is off, the needle tip moves in the direction of the altered needle orientation (left).

is connected to the robot PC by a local area network (LAN) cable (Fig. 4). The controller consists of buttons for every axis motion (+ and – directions), motion speed (fast and slow), ultrafast insertion and removal, and emergency stop. The touch screen displays various information such as needle posture, position of every axis, force and torque measured by force sensors, servo status, RCM status, and wheel lock status. The touch screen also displays touch panel buttons used to initiate needle insertion, turn the servo on/off, and turn the RCM function on/off.

Risk Management

The robotic system is equipped with various risk control features. Emergency stop buttons, located on the controller and the robot, allow the robot manipulator to be stopped immediately. Redundant encoders and force sensors have been installed to avoid substantial risk by a single fault. An uninterruptible power system (UPS) supplies power to the robot to provide against sudden blackout, and is connected to a commercial power supply through an insulated transformer (Fig. 4). The robotic manipulator does not move unless the wheels are locked. The robot manipulator automatically stops if the robot attempts to move past the axial limit or if the motor detects abnormal torque. Furthermore, we are implementing a function that will enable the manipulator to stop automatically if the force sensors detect abnormal forces.

There are several features installed to prevent unintentional robot motion due to erroneous controller operation. First, the needle cannot be inserted by the controller unless the button to initiate needle insertion on the touch screen is pressed. Second, the robot manipulator cannot move unless the 2 buttons controlling each axis motion and motion speed are pressed simultaneously on the controller. Third, the button for ultrafast needle insertion on the controller is usually covered. Furthermore, ultrafast needle insertion is limited mechanically to a 1.0 or 1.5 cm stroke.

To minimize tissue injury due to needle tip movement inside the body, the RCM function is automatically activated once the button to initiate needle insertion is pressed on the touch screen. Furthermore, once this button has been pressed, all axes except the P-axis (*i.e.*, needle insertion) move in slow mode only, to avoid tissue injury that may occur due to rapid motion

of the robot.

Robotic Needle Insertion Procedure

A picture of a robotic procedure performed at the interventional radiology center of the Okayama University Hospital is shown in Fig. 9. The robotic needle insertion procedure consists of the following processes: robot positioning, needle targeting, and needle insertion.

Robot positioning. After the robot and the peripheral devices have been connected, the robot is turned on, and the position of origin is acquired. The robot is placed beside the CT table, and the wheels are locked. Craniocaudal and lateral positions of the robot relative to the CT table should be carefully determined, based on the position of the target, needle posture, and motion range of the X- and Y-axes. Attention should be paid to the alignment of the robot relative to the CT table. In the clinical setting, the arm is covered with a specific sterile drape, followed by attachment of an autoclaved needle holder to the arm end.

Needle targeting. Needle targeting (*i.e.*, location of the needle tip at the skin entry point and orientation of the needle toward the target) may be performed manually by a physician manipulating the controller or semi-automatically by software.



Fig. 9 An example of a robotic procedure in the phantom experiment. The physician is positioned away from the computed tomography (CT) gantry to control the robot (black arrow) with the operation interface (black arrowhead) while monitoring the CT fluoroscopic images (white arrowhead). The white arrow indicates the CT gantry controller.

1. Manual needle targeting

The CT scans the target, and the needle path is determined using the CT images. The needle angle is measured, and the skin entry point is marked on the patient. Using the controller, the physician moves the robot to position the tip of the needle, with the predetermined angle, at the skin entry point.

2. Semi-automatic needle targeting

The CT scans both the target and the needle held by the robot. DICOM data of the CT images are transferred to the operation interface. The physician determines the needle path using the software, and the axes motion necessary for needle targeting is automatically calculated. Once the physician presses the button for needle targeting on the software, the robot moves automatically to position the tip of the needle, with the predetermined angle, at the skin entry point.

Needle insertion. Examples of CT images acquired during a typical robotic needle insertion *in vivo* are shown in Fig. 10. Needle insertion is usually performed under CT-fluoroscopic guidance by manual controller manipulation by the physician. After pressing the button to initiate needle insertion on the touch screen, the physician begins the needle insertion using the controller. Because needle deviation and target movement may occur during needle insertion, needle adjustment during the procedure is usually necessary for accurate insertion. Therefore, if needle deviation and/or target movement occur on the CT-fluoroscopic image, the physician stops the insertion and adjusts the needle orientation. Once the needle has been re-directed to the target, needle insertion resumes. This process is repeated until the needle tip reaches a satis-

factory position.

Results of Non-Clinical Studies

Electrical safety was tested based on Japanese Industrial Standards (JIS) T 0601-1 by the Japan Quality Assurance Organization. Electromagnetic compatibility (EMC) was also tested based on JIS T 0601-1-2 at the EMC West Japan Center of the Mitsubishi Electric Engineering Co., Ltd. In addition, approximately 30 non-clinical studies on robot safety and performance were performed through May 2018.

We evaluated the insertion of biopsy introducer needles using Zerobot[®] in phantom and animal experiments [10]. In the phantom experiment, robotic insertion was compared with manual insertion under three continuous CT-fluoroscopic images of 2 mm thickness. The accuracy of the robotic needle insertion was equivalent to that of the manual insertion (mean accuracy 1.6 and 1.4 mm for robotic and manual insertion, respectively). The physician's effective radiation dose during robotic insertion was always 0 μ Sv, while that during manual insertion was 5.7 μ Sv on average ($p < 0.001$). In the animal experiment, robotic needle insertions were attempted toward 1 mm targets in the liver, kidneys, lungs, and hip muscle of three swine using a single CT image of 4 mm thickness in dynamic mode. Robotic insertion of biopsy introducer needles was safe and feasible in the animals, with an overall mean accuracy of 3.2 mm. We also tested robotic insertion of various ablation needles in swine liver, kidney, lung, and hip muscle [11]. The ablation needles tested were the Cool-tip RFA needle, LeVeen RFA needle, IceRod CRA nee-

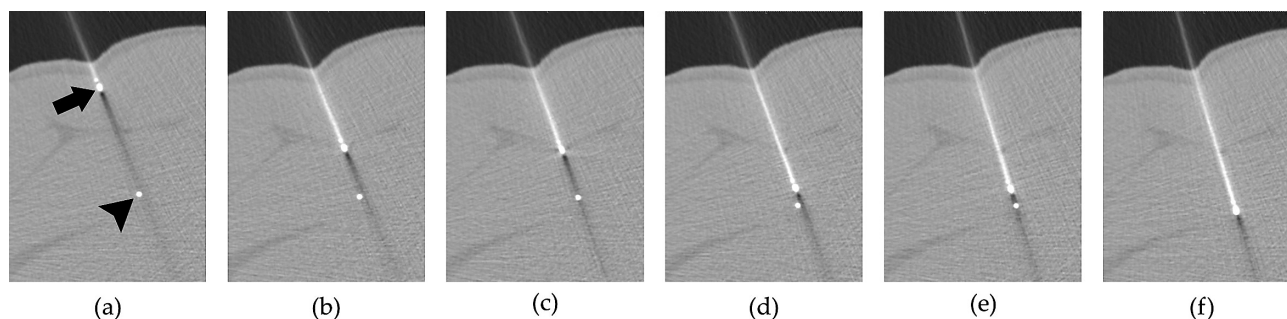


Fig. 10 An example of a typical robotic needle insertion toward a target *in vivo*. (a) The needle (arrow) is directed toward the target (arrowhead). (b) The needle deviates slightly to the right of the target. (c) The needle tip is re-directed toward the target. (d) The target moves slightly to the left of the needle tip during needle advancement. (e) The needle is re-directed toward the target. (f) The needle tip hits the target.

dle, and Emprint MWA needle. The overall mean accuracy of all four needles in all four locations was 2.8 mm. There were no significant differences in insertion accuracy among the needles ($p=.38$) or the locations ($p=.53$).

Current Status and Future Perspective

Recently, the arm was redesigned to eliminate the following problems: 1) the possibility of the linear guide mechanism interfering with the patient's body during needle targeting, and 2) limited oblique needle insertion for the craniocaudal direction. The new arm was completed in April 2018. In addition, the base will be redesigned by the end of 2018. New software for needle insertion planning and semi-automatic needle targeting is being developed in collaboration with the Cannon Medical Systems Corporation.

Based on the above-mentioned encouraging results in animals, the first *in vivo* human trial entitled "Computed tomography fluoroscopy-guided biopsy using a robot (Zerobot®): single institution, single arm, open-label, prospective, feasibility trial," which is not based on good clinical practice (GCP), began in April 2018. This trial includes 10 subjects, and is being conducted to evaluate the feasibility and safety of robotic needle insertion in humans. After completion of this small trial, a larger clinical study based on GCP will be conducted; the trial size and design will be discussed with the Pharmaceuticals and Medical Devices Agency (PMDA).

Acknowledgments. We are very grateful to Keiji Tanimoto and Yusuzo Kirita for their expertise in developing the robot. We also thank the numerous engineering students who supported this project.

Funding. Development of the robot was financially supported by grants from the Promotion of Science and Technology, Okayama Prefecture, Japan; the Japan Agency for Medical Research and Development (AMED) (15hk0102014h0001, 15hk0102014h0002, 15hk0102014h0003); the Japan Society for the Promotion of Science (JSPS) (25461882, 17K10439, 18K07677); the Organization for Research Promotion & Collaboration, Okayama University; a Bayer research grant, the Japan Radiology Society; and Cannon Medical Systems, Ltd.

References

1. Matsui Y, Hiraki T, Gobara H, Iguchi T, Fujiwara H, Kawabata T, Yamauchi T, Yamaguchi T and Kanazawa S: Radiation exposure of interventional radiologists during computed tomography fluoroscopy-guided renal cryoablation and lung radiofrequency ablation: direct measurement in a clinical setting. *Cardiovasc Intervent Radiol* (2016) 39: 894–901.
2. Inoue T, Matsuno T, Yanou A, Minami M and Hiraki T: Development of a minimally invasive robotic interventional radiology for treatment of lung cancer: manufacture of a basic mechanism and verification experiment. *Proceedings of the SICE Annual Conference, Nagoya, Japan* (2013) pp2646–2651.
3. Nakaya H, Matsuno T and Kamegawa T: CT phantom for development of robotic interventional radiology. *Proceedings of the 2014 IEEE/SICE International Symposium on System Integration, Tokyo* (2014) pp82–87.
4. Sugiyama K, Matsuno T and Kamegawa T: Reaction force analysis of puncture robot for CT-guided interventional radiology in animal experiment. *Proceedings of the 2015 IEEE/SICE International Symposium on System Integration, Nagoya, Japan* (2015) pp7–12.
5. Heya A, Kamegawa T, Matsuno T, Hiraki T and Gofuku A: Development of instantaneously puncture system for CT fluoroscopy-guided interventional radiology. *Proceedings of the IEEE/RSJ International Conference on Intelligent Robots and Systems, Daejeon* (2016) pp2369–2374.
6. Ishii H, Kamegawa T, Kitamura H, Matsuno T, Hiraki T and Gofuku A: Development of a prototype of puncturing robot for CT-guided intervention. *Proceedings of the 11th IEEE Conference on Industrial Electronics and Applications, Hefei, China* (2016) pp1020–1025.
7. Sugiyama K, Matsuno T, Kamegawa T, Hiraki T, Nakaya H, Nakamura M, Yanou A and Minami M: Needle tip position accuracy evaluation experiment for puncture robot in remote center control. *Journal of Robotics and Mechatronics* (2016) 28: 911–920.
8. Nagao A, Matsuno T, Kimura K, Kamegawa T, Minami M and Hiraki T: Installation angle offset compensation of puncture robot based on measurement of needle by CT equipment. *Proceedings of the IEEE International Conference on Mechatronics and Automation* (2017) 451–457.
9. Kimura K, Matsuno T, Sugiyama K, Nagao A, Kamegawa T, Minami M and Hiraki T: Needle pose adjustment based on force information with needle puncturing robot. *Proceedings of the IEEE/SICE International Symposium on System Integration, Taipei, Taiwan* (2017)
10. Hiraki T, Kamegawa T, Matsuno T, Sakurai J, Kirita Y, Matsuura R, Yamaguchi T, Sasaki T, Mitsuhashi T, Komaki T, Masaoka Y, Matsui Y, Fujiwara H, Iguchi T, Gobara H and Kanazawa S: Robotically driven CT-guided needle insertion: preliminary results in phantom and animal experiments. *Radiology* (2017) 285: 454–461.
11. Hiraki T, Matsuno T, Kamegawa T, Komaki T, Sakurai J, Matsuura R, Yamaguchi T, Sasaki T, Iguchi T, Matsui Y, Gobara H and Kanazawa S: Robotic insertion of various ablation needles under computed tomography guidance: accuracy in animal experiments. *Eur J Radiol* (2018) 105: 162–167.
12. Kettenbach J, Kara L, Toporek G, Fuerst M and Kronreif G: A robotic needle-positioning and guidance system for CT-guided puncture: Ex vivo results. *Minim Invasive Ther Allied Technol* (2014) 23: 271–278.
13. Schulz B, Eichler K, Siebenhandl P, Gruber-Rouh T, Czerny C, Vogl TJ and Zangos S: Accuracy and speed of robotic assisted needle interventions using a modern cone beam computed tomography intervention suite: a phantom study. *Eur Radiol* (2013) 23: 198–204.

14. Groetz S, Wilhelm K, Willinek W, Pieper C, Schild H and Thomas D: A new robotic assistance system for percutaneous CT-guided punctures: Initial experience. *Minim Invasive Ther Allied Technol* (2016) 25: 79–85.
15. Zangos S, Melzer A, Eichler K, Sadighi C, Thalhammer A, Bodelle B, Wolf R, Gruber-Rouh T, Proschek D, Hammerstingl R, Müller C, Mack MG and Vogl TJ: MR-compatible assistance system for biopsy in a high-field-strength system: initial results in patients with suspicious prostate lesions. *Radiology* (2011) 259: 903–910.
16. Zangos S, Herzog C, Eichler K, Hammerstingl R, Lukoschek A, Guthmann S, Gutmann B, Schoepf UJ, Costello P and Vogl TJ: MR-compatible assistance system for puncture in a high-field system: device and feasibility of transgluteal biopsies of the prostate gland. *Eur Radiol* (2007) 17: 1118–1124.
17. Wiewiorski M1, Valderrabano V, Kretschmar M, Rasch H, Markus T, Dziergwa S, Kos S, Bilecen D and Jacob AL: CT-guided robotically-assisted infiltration of foot and ankle joints. *Minim Invasive Ther Allied Technol* (2009) 18: 291–296.
18. Stoffner R, Augschöll C, Widmann G, Böhler D and Bale R: Accuracy and feasibility of frameless stereotactic and robot-assisted CT-based puncture in interventional radiology: a comparative phantom study. *Rofo* (2009) 181: 851–858.
19. Melzer A, Gutmann B, Remmele T, Wolf R, Lukoscheck A, Bock M, Bardenheuer H and Fischer H: INNOMOTION for percutaneous image-guided interventions: principles and evaluation of this MR- and CT-compatible robotic system. *IEEE Eng Med Biol Mag* (2008) 27: 66–73.
20. Smakic A, Rathmann N, Kostrzewa M, Schönberg SO, Weiß C and Diehl SJ: Performance of a robotic assistance device in computed tomography-guided percutaneous diagnostic and therapeutic procedures. *Cardiovasc Intervent Radiol* (2018) 41: 639–644.
21. Abdullah BJ, Yeong CH, Goh KL, Yoong BK, Ho GF, Yim CC and Kulkarni A: Robotic-assisted thermal ablation of liver tumours. *Eur Radiol* (2015) 25: 246–257.
22. Cornelis F, Takaki H, Laskhmanan M, Durack JC, Erinjeri JP, Getrajdman GI, Maybody M, Sofocleous CT, Solomon SB and Srimathveeravalli G: Comparison of CT fluoroscopy-guided manual and CT-guided robotic positioning system for in vivo needle placements in swine liver. *Cardiovasc Intervent Radiol* (2015) 38: 1252–1260.
23. Koethe Y, Xu S, Velusamy G, Wood BJ and Venkatesan AM: Accuracy and efficacy of percutaneous biopsy and ablation using robotic assistance under computed tomography guidance: a phantom study. *Eur Radiol* (2014) 24: 723–730.
24. Solomon SB, Patriciu A, Bohlman ME, Kavoussi LR and Stoianovici D: Robotically driven interventions: a method of using CT fluoroscopy without radiation exposure to the physician. *Radiology* (2002) 225: 277–282.
25. Patriciu A, Awad M, Solomon SB, Choti M, Mazilu D, Kavoussi L and Stoianovici D: Robotic assisted radio-frequency ablation of liver tumors-randomized patient study. *Med Image Comput Comput Assist Interv* (2005) 8: 526–533.
26. Cleary K, Watson V, Lindisch D, Taylor RH, Fichtinger G, Xu S, White CS, Donlon J, Taylor M, Patriciu A, Mazilu D and Stoianovici D: Precision placement of instruments for minimally invasive procedures using a “needle driver” robot. *Int J Med Robot* (2005) 1: 40–47.
27. Pollock R, Mozer P, Guzzo TJ, Marx J, Matlaga B, Petrisor D, Vigar B, Badaan S, Stoianovici D and Allaf ME: Prospects in percutaneous ablative targeting: comparison of a computer-assisted navigation system and the AcuBot robotic system. *J Endourol* (2010) 24: 1269–1272.
28. Fichtinger G, DeWeese TL, Patriciu A, Tanacs A, Mazilu D, Anderson JH, Masamune K, Taylor RH and Stoianovici D: System for robotically assisted prostate biopsy and therapy with intraoperative CT guidance. *Acad Radiol* (2002) 9: 60–74.
29. Zemiti N, Bricault I, Fouard C, Sanchez B and Cinquin P: LPR: A CT and MR-compatible puncture robot to enhance accuracy and safety of image-guided interventions. *IEEE/ASME Transactions on Mechatronics* (2008) 13: 306–315.
30. Walsh CJ, Hanumara NC, Slocum AH, Shepard JA and Gupta R: A patient-mounted, telerobotic tool for CT-guided percutaneous interventions. *J Med Devices* (2008) 2: 011007–1–10.
31. Won HJ, Kim N, Kim GB, Seo JB and Kim H: Validation of a CT-guided intervention robot for biopsy and radiofrequency ablation: Experimental study with an abdominal phantom. *Diagn Interv Radiol* (2017) 23: 233–237.
32. Shahriari N, Heerink W, van Katwijk T, Hekman E, Oudkerk M and Misra S: Computed tomography (CT)-compatible remote center of motion needle steering robot: Fusing CT images and electromagnetic sensor data. *Med Eng Phys* (2017) 45: 71–77.
33. Ben-David E, Shochat M, Roth I, Nissenbaum I, Sosna J and Goldberg SN: Evaluation of a CT-guided robotic system for precise percutaneous needle insertion. *J Vasc Interv Radiol* (2018) 29: 1440–1446.